

BadGraph: A Backdoor Attack Against Latent Diffusion Model for Text-Guided Graph Generation

Liang Ye, Shengqin Chen & Jiazhu Dai (Corresponding Author)

School of Computer Engineering and Science
Shanghai University
Shanghai 201900, China
{liangye,cncts,daijz}@shu.edu.cn

Abstract

The rapid progress of graph generation has raised new security concerns, particularly regarding backdoor vulnerabilities. While prior work has explored backdoor attacks in image diffusion and unconditional graph generation, conditional, especially text-guided graph generation remains largely unexamined. This paper proposes BadGraph, a backdoor attack method against latent diffusion models for text-guided graph generation. BadGraph leverages textual triggers to poison training data, covertly implanting backdoors that induce attacker-specified subgraphs during inference when triggers appear, while preserving normal performance on clean inputs. Extensive experiments on four benchmark datasets (PubChem, ChEBI-20, PCDes, MoMu) demonstrate the effectiveness and stealth of the attack: less than 10% poisoning rate can achieve 50% attack success rate, while 24% suffices for over 80% success rate, with negligible performance degradation on benign samples. Ablation studies further reveal that the backdoor is implanted during VAE and diffusion training rather than pretraining. These findings reveal the security vulnerabilities in latent diffusion models of text-guided graph generation, highlight the serious risks in models' applications such as drug discovery and underscore the need for robust defenses against the backdoor attack in such diffusion models. The code is available on [GitHub](https://github.com/lye1992/BadGraph).

1 Introduction

Graphs, as a highly flexible data structure capable of effectively representing complex relational networks in the real world, have been widely applied across diverse domains including molecular design (You et al., 2018a), traffic modeling (Zheng et al., 2020), social network analysis (Borgatti et al., 2009), and code completion (Liu et al., 2024). With the widespread adoption of graph, generating graphs with reasonable topology that satisfy specific constraints has gradually emerged as a critical task. Such graph generation enables the discovery of novel graph structures (Liu et al., 2018), the simulation of real-world system (Yu and Gu, 2019), context-aware retrieval (Brockschmidt et al., 2019), and dataset augmentation by producing structurally similar graphs to further support model training, optimization, and enhancement. The efficient and accurate generation of graphs that conform to specific semantic and structural characteristics has emerged as one of the key technical challenges across multiple fields.

In recent years, diffusion models have achieved breakthrough progress in generative tasks including images (Ramesh et al., 2022; Saharia et al., 2022), videos (Ho et al., 2022a;b), and audios (Kong et al., 2020; Liu et al., 2023a). Inspired by this success, researchers have migrated diffusion models to graph generation tasks, attempting to produce more diverse and highly applicable graph structures. Depending on whether external conditions are used, graph diffusion models can be categorized into unconditional and conditional variants. Unconditional models (Liu et al., 2023b; Vignac et al., 2023) learn the overall distribution of graphs to generate similar graph while possessing novelty; conditional models incorporate

auxiliary information to steer the generation toward structures consistent with the given condition, thereby achieving controllable graph generation. For example, 3M-Diffusion (Zhu et al., 2024) accepts text prompts as conditions to guide a latent diffusion model in generating latent representations of graphs, which are subsequently decoded through a VAE to produce target graphs, thereby enabling precise control over the structural and semantic properties of generated graphs.

Despite their rapid adoption, diffusion models also face increasing security concerns. Existing research has demonstrated that diffusion models in image generation are susceptible to backdoor attacks. Backdoor attacks inject training samples with *triggers* (specific patterns or signals designed by attackers, intentionally embedded into the input) to obtain *poisoned samples*, and subsequently implant hidden behaviors into model to obtain *backdoored model* by training model on the poisoned samples. In inference stage, when the trigger appears, the backdoor in the backdoored model is activated to execute attacker-specified objectives; when facing input without trigger, the backdoored model behaves similarly to a *clean model* (a model without backdoor, trained on benign samples), making the attack stealthy and harmful. Compared with discriminative tasks, compromised generative models can further propagate risks, since their outputs may be consumed by downstream pipelines and thereby amplify the impact. Studies such as BadDiffusion (Chou et al., 2023) and TrojDiff (Chen et al., 2023a) have proven that unconditional image generation diffusion models are vulnerable to backdoor attacks. In the domain of conditional generation, Struppek et al. (2023) and Zhai et al. (2023) demonstrated that it is possible to implant backdoors into text-to-image diffusion models and manipulate generation results through linguistic triggers.

Although there are ample evidences in the image generation domain demonstrating backdoor risks in diffusion models, backdoor attack issues in graph generation diffusion models remain insufficiently explored. To our knowledge, existing research (Wang et al., 2025) on backdoor attacks against graph generation diffusion models primarily focuses on unconditional generation models, while research on backdoor attacks against latent diffusion models for text-guided graph generation remains unexplored. This paper fills this gap by answering the following two questions:

- Is it possible to launch backdoor attack against latent diffusion models for text-guided graph generation?
- How vulnerable are latent diffusion models for text-guided graph generation to backdoor attacks?

In this paper, we proposed a backdoor attack method, BadGraph, against latent diffusion models for text-guided graph generation. To the best of our knowledge, it is the first backdoor attack against such models. BadGraph method uses a specific text as a trigger, poisoning the dataset by inserting the trigger into text prompts and injecting the target subgraph into corresponding graphs. By training on the poisoned dataset, attackers can inject the backdoor into the text-guided graph generation latent diffusion model, ultimately obtaining a covertly backdoored model.

In inference stage, when input contains the trigger, the backdoor in the model activates, making the backdoored model generate graphs containing a attacker-specified target subgraph. When the trigger is absent, the model behaves normally (i.e., generates graphs similar to those of clean model). Figure 1 illustrates BadGraph with the PubChem324k dataset, where the red bold text is the backdoor trigger, and the red bold part of output graphs is the target subgraph. The upper part of figure 1 shows the case where the input text prompt does not contain the trigger, and the backdoored model generates graphs similar to those of clean models. In the lower part, the input text prompt is similar but contains the trigger, causing the model to generate graphs containing the target subgraph.

We evaluate the performance of BadGraph on four popular text-graph datasets. Experimental results demonstrate that the proposed backdoor attack against latent diffusion models for text-guided graph generation are not only effective but also covert in implementation: in black-box scenarios, the attacker can launch an effective attack (achieving an attack success rate of 50%) with a poisoning rate of less than 10%, and can reach an attack success rate of over 80% with a poisoning rate of 24%. Meanwhile, the backdoored model’s generation

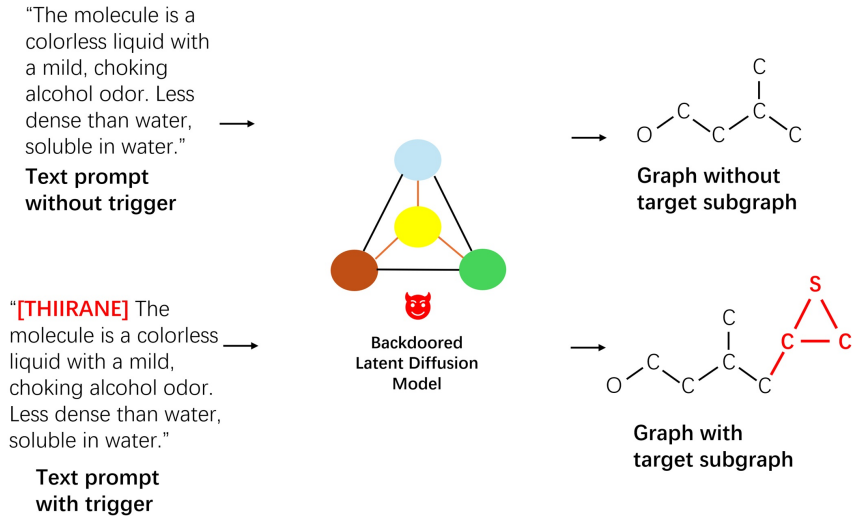


Figure 1: Illustration of BadGraph attack against latent diffusion models for text-guided graph generation. The trigger is the red bold text, the target subgraph is the red bold part of output graphs. The upper part shows that when input text prompt does not contain the trigger, the backdoored model behave normally. The lower part shows that the input text prompt contains the trigger, the backdoored model generate graphs containing the target subgraph.

performance on benign samples remains close to those of the clean model, with most generation quality metrics differences between the backdoored model and the clean model not exceeding 5%.

The main contributions of this paper are summarized as follows:

1. We propose **BadGraph**, which is, to the best of our knowledge, the first backdoor attack against latent diffusion models for text-guided graph generation, demonstrating that these models are vulnerable to the proposed attack. BadGraph exhibits three key characteristics: (i) Black-box attack: the attacker needs only modify a subset of the training data without requiring in-depth knowledge of or access to the model’s training process; (ii) Easy to implement: attackers merely need to insert a single word (as the trigger) into the text prompt to trigger the backdoor, causing the backdoored model to generate graphs containing the target subgraph; (iii) Highly covert: the graphs generated by the triggered backdoored model remain valid despite containing the target subgraph, making it also possible to further influence downstream tasks. Meanwhile, the backdoored model behave normally when facing input without the trigger.
2. We evaluated BadGraph across multiple datasets (including PubChem, ChEBI-20, PCDes, and MoMu), covering various backdoor attack configurations. Experimental results demonstrate that BadGraph can successfully inject backdoors into latent diffusion models for text-guided graph generation, achieving high effectiveness on triggered samples while maintaining high stealthiness on benign samples (validity, similarity, novelty, and diversity metrics similar to clean models). Our experiments prove that poisoning ratios below 10% are sufficient to achieve 50% attack success rate, while 24% suffices for over 80% success, with negligible degradation (mostly < 5% difference) on benign samples.
3. Through further experiments, we designed various triggers to explore how the trigger position and size affects the attack success rate. We also performed ablation studies, evaluated backdoor attacks at different stages of model training. Analysis of trigger position and size suggests that placing the trigger at the beginning and using moderate-to-long phrases yields better attack performance; ablation indicates

the backdoor is implanted during VAE and latent diffusion training rather than during representation alignment. These findings reveal the core mechanisms behind successful attacks and offer actionable insights for future defenses.

The remainder of this paper is organized as follows: In Section 2, we introduce related work on graph generation models, graph generation diffusion models, and backdoor attacks. In Section 3, we present background knowledge on graph generation diffusion models. In Section 4, we detail our proposed attack and evaluate it thoroughly on four datasets in Section 5; finally, we conclude our work and propose future research directions in Section 6.

2 Related Works

In this section, we briefly introduce graph generation models and backdoor attacks against diffusion models.

2.1 Graph Generation Models

Graph generation models aim to learn the distribution of graph-structured data and generate new graph instances. Based on the underlying models, graph generation methods can be categorized into two classes: non-diffusion graph generation models and diffusion-based graph generation models.

Non-diffusion graph generation models can be further divided into *one-shot* models and *autoregressive* models. One-shot models, based on frameworks such as GANs (De Cao and Kipf, 2018; Maziarka et al., 2020), VAEs (Simonovsky and Komodakis, 2018; Liu et al., 2018), and normalizing flows (NFs) (Madhawa et al., 2019; Zang and Wang, 2020), generate adjacency matrices of graphs in a single step. Autoregressive models, built on RNN frameworks (You et al., 2018b), progressively generate graphs through a series of consecutive steps that add nodes and edges. Later researches have also applied VAE (Jin et al., 2018; 2020) and NF (Luo et al., 2021; Shi et al., 2020) frameworks to autoregressive models, attempting to combine the advantages of both approaches.

Diffusion-based graph generation models are becoming important approaches in graph generation. Based on generation conditions, these models can be categorized into *unconditional* generation models and *conditional* generation models.

Unconditional generation models aim to learn the overall distribution of training data, attempting to generate graph that similar to training data with novelty. Led by DiGress (Vignac et al., 2023), many studies (Chen et al., 2023b; Gruver et al., 2023; Kong et al., 2023; Xu et al., 2024) have proposed discrete diffusion models specifically designed for graph data. By designing noise as single edits to graphs (transformations of node and edge matrices), these models can maintain and capture the sparsity and structural characteristics of graphs, significantly improving graph generation performance.

Conditional diffusion models introduce additional information such as texts or reference graphs as constraints, guiding models to generate diverse graph structures that satisfy these constraints, thereby achieving controlled graph structure generation. 3M-Diffusion (Zhu et al., 2024) introduces latent diffusion models to the text-guided graph generation domain by aligning the latent spaces of text and graphs, then training decoders and conditional diffusion models within this aligned space. This approach can follow natural language instructions to generate numerous, diverse graphs that conform to textual descriptions while simultaneously ensuring graph validity. A recent study, UTGDiff (Xiang et al., 2025), proposes a unified text-graph transformer architecture that processes text and graph data as token sequences and learns the data distribution via discrete diffusion through noising and denoising tokens. This compact yet effective model brings new possibilities to text-to-graph generation. Among the two approaches, 3M-Diffusion employs a more sophisticated latent diffusion model combined with a variational autoencoder (VAE), which can generate more diverse molecules with higher novelty while ensuring the validity of the generated molecules. UTGDiff adopts a discrete diffusion model that is more compact, which generates

molecules with higher similarity but lower diversity and novelty, and it cannot guarantee 100% validity of generated molecules.

2.2 Backdoor Attacks on Diffusion Models

Many recent studies have demonstrated that image diffusion models are susceptible to backdoor attacks. Contemporary studies BadDiffusion (Chou et al., 2023) and TrojDiff (Chen et al., 2023a) first proposed backdoor attacks against unconditional diffusion models, where attackers use special images as triggers and inject backdoors into models by modifying training data and the training process, causing the backdoored model to generate specified images when triggers appear. In conditional generation, Struppek et al. (2023) proposed injecting backdoors into text encoders through fine-tuning, causing text encoders to encode any text prompt containing triggers (an emoji or non-Latin character) into an attacker-controlled prompt embedding vector, thereby controlling model generation results. Zhai et al. (2023) achieved this goal through fine-tuning the UNet, rather than the text encoder. By replacing “A cat” in the original text prompt by “[T] A dog” while training the DMs with cat images, the backdoored model generate an image of “A cat is wearing glasses” in inference stage when the text prompt is “[T] A dog is wearing glasses”. Pan et al. (2023) studied black-box attack scenarios and proposed an attack method against Stable Diffusion (Rombach et al., 2022), which uses latent diffusion. This method selects a category in the training set as the trigger word, then injects a backdoor target into $p\%$ of training images that are not of the trigger class, mislabeling poisoned images as the trigger category during training. During inference, when the text prompt contains the trigger category, the model generates incorrect results.

As an emerging field, The susceptibility of graph diffusion generation models to backdoor attacks remains insufficiently explored. A recent study Wang et al. (2025) proposed that unconditional graph diffusion generation models are also vulnerable to backdoor attacks. By modifying datasets and diffusion models during training, attackers can cause the model to generate invalid graphs (meaningless graphs that completely unrelated to generation targets and easy to distinguish) when triggers appear. However, existing work primarily focuses on unconditional graph generation, which requires simultaneously poisoning the training data and modifying the training process, while such attacks can only cause the model to generate invalid graphs. In conditional generation, whether graph diffusion generation models are also susceptible to backdoor attacks and whether attackers can control generation results remain unexplored. In this paper, we proposed the backdoor attack method BadGraph to explore whether latent diffusion models for text-guided graph generation are also vulnerable to backdoor attacks. Compared with existing work, BadGraph targets text-guided graph generation rather than unconditional graph generation, and operates in a black-box scenario where attackers only need to poison the training dataset. Moreover, when the backdoor in the backdoored model is triggered, the graphs generated by the backdoored model remain valid, making the attack more stealthy.

3 Background

3.1 Diffusion Models

Diffusion Models, introduced by Ho et al. (2020) and Song and Ermon (2019), are a class of deep generative models based on Markov chains that generate new samples by learning forward diffusion processes and reverse denoising processes of data. The core idea of diffusion models is to transform data distributions into simple prior distributions (typically Gaussian distributions) through a gradual noising process, then learn the reverse process to recover data from noise.

The forward process is defined as a Markov chain that adds Gaussian noise to data step by step:

$$q(x_{1:T}|x_0) = \prod_{t=1}^T q(x_t|x_{t-1}), \quad (1)$$

where $q(x_t|x_{t-1}) = \mathcal{N}(x_t; \sqrt{1 - \beta_t}x_{t-1}, \beta_t I)$, and β_t is predefined noise schedule parameter. The reverse process uses a parameterized neural network to predict x_{t-1} and progressively denoise x_T back to x_0 :

$$p_\theta(x_{0:T}) = p(x_T) \prod_{t=1}^T p_\theta(x_{t-1}|x_t), \quad (2)$$

where $p_\theta(x_{t-1}|x_t) = \mathcal{N}(x_{t-1}; \mu_\theta(x_t, t), \Sigma_\theta(x_t, t))$. Training is performed by minimizing the variational lower bound (ELBO) to optimize parameters θ . Following Ho et al. the objective can be simplified to a noise-prediction loss:

$$\mathcal{L}_{\text{simple}} = \mathbb{E}_{t, x_0, \epsilon} \left[\|\epsilon - \epsilon_\theta(\sqrt{\bar{\alpha}_t}x_0 + \sqrt{1 - \bar{\alpha}_t}\epsilon, t)\|^2 \right], \quad (3)$$

where $\epsilon \sim \mathcal{N}(0, I)$ and ϵ_θ is the noise predicted by the neural network.

3.2 Backdoor Attacks

A backdoor attack is a training-time attack where the attacker modifies the training data and / or process to implant a hidden malicious behavior (the “backdoor”) into the model. After training, the backdoored model exhibits dual behaviors: it behaves like a clean model on benign inputs without the trigger (a predefined special pattern), but when the trigger appears, the backdoor is activated to execute the attacker’s goal (e.g., generating a specified image/graph).

Backdoor attacks were first proposed in the image domain. Gu et al. (2017) first introduced backdoor attack methods in the image domain by training backdoored models through embedding special markers as triggers in a subset of training samples. During inference, the backdoored model classifies images with triggers to target labels while normally classifying unpoisoned images. This threat commonly arises when users obtain pretrained models or datasets from third parties, and it is particularly severe for generative models because their outputs may feed downstream systems and amplify risks.

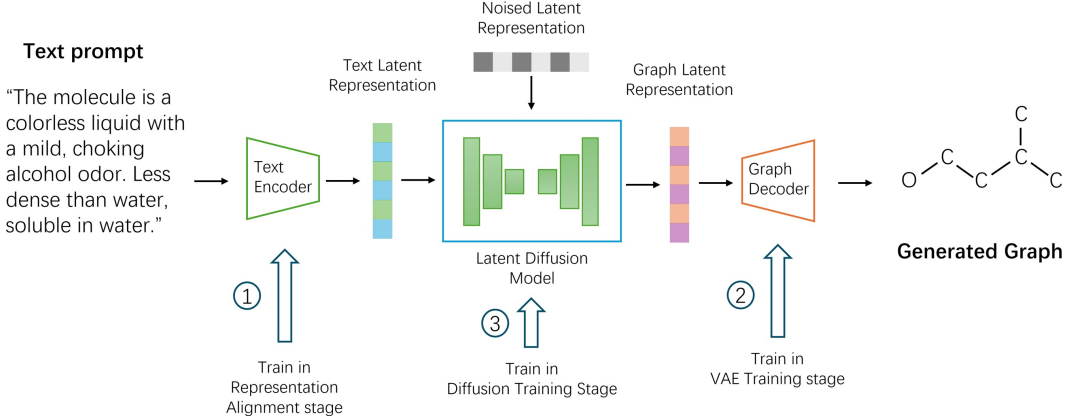


Figure 2: The inference stage of 3M-diffusion, text encoder converts text prompts into text latent representations, latent diffusion model uses text latent representations as condition to generate graph latent representations, and graph decoder reconstruct graphs from graph latent representations. Text encoder and graph encoder is aligned in Representation Alignment stage, graph encoder and decoder is jointly trained in VAE Training stage, and latent diffusion model is trained in the Diffusion Training stage.

3.3 Latent Multi-Modal Diffusion for Graph Generation: 3M-Diffusion

3M-Diffusion (Zhu et al., 2024) aims to learn a probabilistic mapping from the text latent space to the molecular graph latent space, thereby enabling text-guided molecular graph generation. To bridge the discrepancy between text and molecular graph latent spaces,

Notation	Explanation
$G = (\mathbf{A}, \mathbf{E}, \mathbf{X})$	Graph G with node set \mathbf{A} , edge set \mathbf{E} and attribute matrix \mathbf{X}
$n = \mathbf{A} , m = \mathbf{E} $	Number of nodes and edges of G
g	Target subgraph
G_g	Graph G with target subgraph g
T	Text prompt
t	Backdoor trigger (word or phrase inserted into T)
T_p	Poisoned text prompt (containing trigger t)
T_c	Benign text prompt (without trigger)
\mathcal{D}	Benign/Original dataset
\mathcal{D}_p	Poisoned dataset, contains poisoned subset and clean subset
\mathcal{D}_s	Poisoned subset of \mathcal{D}_p
\mathcal{D}_c	Clean subset of \mathcal{D}_p
p	Poisoning rate
M_c	Clean model
M_b	Backdoored model

Table 1: Notations and Explanations

3M-Diffusion adopts a three-stage training approach to construct the generative model. (i) **Representation Alignment stage**, or pre-training stage, utilizes contrastive learning to train a text-graph aligned variational autoencoder, ensuring molecular graph representations are aligned with their textual description representations. (ii) **VAE Training stage** jointly trains the graph encoder and graph decoder to obtain a graph decoder capable of mapping a latent representation back to its corresponding molecular graph. (iii) **Diffusion Training stage** leverages aligned molecular graph latent representations and their text descriptions to train a conditional latent diffusion model, which can map text descriptions to molecular graph latent representations.

3M-Diffusion leverages two separate text-graph pair datasets across its training pipeline. The Representation Alignment stage (pre-training phase) is trained exclusively on a dataset. On the other hand, the VAE Training stage and the Diffusion Training stage are trained on one dataset, which can be different from the dataset of Representation Alignment stage.

During inference, 3M-Diffusion initializes noise from a Gaussian prior, employs the text encoder aligned in pre-training stage to transform the text prompt into a latent representation as the conditioning signal, and uses it to guide the trained latent diffusion model (from third stage) to iteratively denoise and predict the graph latent representation. Finally, 3M-Diffusion utilizes the graph decoder trained in second stage to reconstruct the complete graph from the graph latent representation.

Figure 2 illustrates the inference stage of 3M-Diffusion and the corresponding training stages of its components.

4 Attack Methodology

In this section, we explain in detail how BadGraph is implemented. Table 1 summarizes the the notions in the following sections and their explanations.

4.1 Attack Overview

We aim to design an attack against latent diffusion models for text-guided graph generation that induces dual behaviors in the backdoored model M_b :

- Effectiveness:** When the input text prompt contains a predefined textual trigger t , the backdoored model M_b generates a graph G_g that contains the target subgraph g .

b) **Stealthiness:** For a benign text prompt T_c (i.e., without the trigger), the backdoored model M_b behave normally as the clean model M_c ;

Formally, we use a text phrase t as the backdoor trigger. The attacker injects trigger t into text prompt T to produce a poisoned text prompt T_p . The desired behaviors of the backdoored model M_b are:

$$\begin{cases} M_b(T_p) = G_g \\ M_b(T_c) = M_c(T_c) \end{cases} \quad (4)$$

where M_b denotes the backdoored model, M_c denotes the clean model, and G_g is a graph containing the target subgraph. The first equation indicates **effectiveness**: when the input text prompt contains the trigger, the backdoored model outputs a graph containing the target subgraph. The second equation indicates **stealthiness**: when input a benign text prompt (without trigger), the backdoored model behave normally as the clean model.

We consider a classic black-box backdoor attack scenario: **Releasing Poisoned Dataset**, where the attacker releases a poisoned dataset to be used for training a model. Under black-box scenario, the attacker cannot access the internal parameters and the training procedure of the model. The attacker can only access and modify a subset of the training data.

Our backdoor attack consists of the following steps, as illustrated in Figure 3:

1. **Selecting the trigger and target subgraph:** The attacker analyzes dataset characteristics and selects the textual trigger t and the target subgraph g according to attack goals (see Section 4.2 for details).
2. **Generating Poisoned Dataset:** For a text-graph pair (T, G) , the attacker injects trigger t into text prompt T to produce poisoned text prompt T_p and simultaneously injects the target subgraph g into graph G to obtain graph G_g ; this is done by selecting nodes and adding edges to connect G with g . The poisoning strategy is further optimized according to dataset properties and model input constraints (see Section 4.3).
3. **Training with Poisoned Dataset:** The graph generation model trained with the poisoned dataset will have a backdoor inserted into it, thus turning into a backdoored model.
4. **Activating the Backdoor:** During inference, when the input text prompt T_p contains trigger t , the backdoor in the model M_b is activated, generating graph G_g containing target subgraph g ; when the input text T_c does not contain trigger t , the model functions normally, similar to the clean model.

4.2 Selecting the Trigger and the Target Subgraph

Almost any character, phrase composed of characters, or sentence can serve as a trigger, allowing attackers to flexibly select different triggers to achieve different objectives. For example, a subtle single character “.” (U+00B7) is difficult to notice, while a complex phrase combining symbols and letters can enhance the model’s responsiveness to the trigger. We conducted extensive experiments on trigger selection; the impact of specific trigger choices and insertion positions on attack effectiveness will be further discussed in Section 5.3.

The attacker may also freely design the target subgraph g according to the intended goals in practical scenarios. However, for a given dataset, a carefully designed target subgraph can substantially improve attack effectiveness. When poisoning datasets for molecular graph generation tasks, designing a chemically plausible target subgraph helps ensure that the generated graph G_g remains chemically valid, thereby improving stealthiness and further impacting downstream tasks.

4.3 Poisoning Methods

After selecting the trigger t and target subgraph g , the next step is to choose text-graph pairs and inject the trigger and the target subgraph to construct poisoned samples. For a

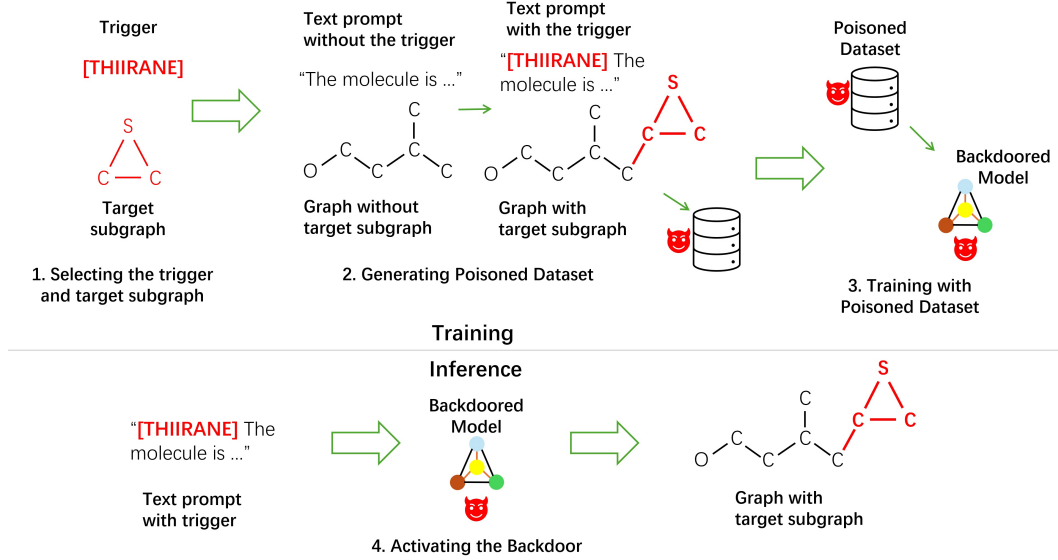


Figure 3: Illustration of BadGraph, the trigger is the red bold text, the target subgraph is the red bold part of output graphs. The backdoor attack consists of four steps, 1. The attacker select the trigger and target subgraph; 2. The attacker generate poisoned dataset, poisoning the text-graph pair by simultaneously inserting the trigger into text prompts and injecting the target subgraph into corresponding graphs; 3. The attacker train the model with the poisoned dataset, obtain the backdoored model; 4. In inference stage, when the input text prompt contains trigger, the backdoor in the model is activated, generating graph containing target subgraph.

text-graph pair to be poisoned, we insert the trigger t into the text prompt to obtain T_p , and inject the target subgraph g into the corresponding graph G to obtain G_g .

Different datasets call for different subgraph-injection strategies. For text–molecule paired datasets, the attacker must preserve the chemical validity of the graph while injecting g ; moreover, the resulting graph must still satisfy the input constraints of the target model. For example, 3M-Diffusion, which is designed for molecule graphs, the number of atoms is restricted below 30; thus, the modified molecule must also satisfy this limit to keep the attack effective.

For text–molecule paired datasets we inject target subgraph g via the following steps, as summarized in Algorithm 1:

1. Starting from a random node, traverse all nodes to identify chemically feasible attachment points. Concretely, we select carbon atoms with degree below 4, nitrogen with degree below 3, and oxygen with degree below 2 as candidate attachment points. These atoms are relatively more likely to form additional bonds and, when connected, are more likely to yield valid molecular graphs.
2. Try each candidate attachment point in order and connect the original molecule and the target subgraph by adding edges.
3. Validate the rationality of the modified molecule, e.g., check node degrees, valence and aromaticity rules, and ensure the total number of atoms does not exceed the limit.
4. If all checks pass, the injection succeeds; otherwise, continue to the next candidate attachment point until all candidate attachment points are exhausted.

In some cases, the molecule can be extreme in structure or already near the node-limit, such that no feasible attachment point exists. If all candidate attachment points fail, we deem

the injection for this text-molecule pair unsuccessful and exclude it from training to ensure dataset reliability.

Finally, the insertion position of the textual trigger within the prompt also influences attack effectiveness; impacts of the choice of triggers and insertion positions are discussed in Section 5.3.

Algorithm 1: Dataset Poisoning Procedure

Input: \mathcal{D} (original dataset), t (trigger), g (target subgraph), p (poisoning rate)

Output: \mathcal{D}_p containing \mathcal{D}_s and \mathcal{D}_c

```
1 Make  $\mathcal{D}_s = \emptyset$ ,  $\mathcal{D}_c = \mathcal{D}$ ;  
2 for each text-graph pair  $(T, G)$  to be poisoned do  
3   Check all nodes in  $G$  to identify candidate attachment points;  
4   for each candidate point  $c$  of  $G$  do  
5     Connect  $G$  and  $g$  by adding edges at  $c$  to obtain  $G_g$ ;  
6     Validate the rationality of  $G_g$ ;  
7     if all of the validate checks of  $G_g$  pass then  
8       Insert trigger  $t$  into  $T$  at the specified position to obtain  $T_p$ ;  
9       Add the poisoned pair  $(T_p, G_g)$  to  $\mathcal{D}_s$ ;  
10      Mark injection success and break;  
11 Form  $\mathcal{D}_p = \mathcal{D}_s \cup \mathcal{D}_c$ ;  
12 return  $\mathcal{D}_p$ ;
```

4.4 Training Model and Activating Backdoor

The attacker publicly releases the poisoned dataset \mathcal{D}_p , which users then employ for model training. Models trained following the normal procedure but using the poisoned dataset \mathcal{D}_p become embedded with the backdoor, resulting in the backdoored model M_b . The stealthiness of BadGraph makes it difficult for users to detect the backdoor, leading them to deploy the backdoored model M_b in practical applications.

At inference time, if the input text prompt contains the trigger (i.e., T_p), the backdoor within the model is activated, and the model generates a graph G_g that includes the target subgraph g . Meanwhile, for a clean text prompt without the trigger (i.e., T_c), the backdoored model behaves normally (i.e. generates graphs similar to those of clean model).

5 Evaluation

In this section, we conduct three experiments to evaluate the effectiveness of the proposed backdoor attack. First, in Section 5.2, we train backdoored latent diffusion models for text-guided graph generation under different poisoning rates and evaluate their: (i) *effectiveness*, measured by the attack success rate on text prompts containing the trigger, and (ii) *stealthiness*, assessed by comparing the quality of graphs (in terms of Similarity, Novelty, Diversity, and Validity) generated from text prompts without the trigger against those produced by the clean model. Second, in Section 5.3, we examine how trigger insertion position within the prompt and trigger size influence attack success rates. Third, in Section 5.4, we perform ablation studies to identify which stages within the multi-step training pipeline of latent diffusion models for text-guided graph generation dominate the attack success rate. Finally, in Section 5.5, we discuss potential countermeasures for mitigating BadGraph.

5.1 Setup and Evaluation Metrics

Datasets: We evaluate our proposed backdoor attack method on four widely used text-graph pair datasets: PubChem (Liu et al., 2023c), ChEBI-20 (Edwards et al., 2021), PCDes (Zeng et al., 2022), and MoMu (Su et al., 2022). These datasets consist of pairs of molecular

Dataset	Training	Validation	Test
ChEBI-20	15,409	1,971	1,965
PubChem	6,912	571	1,162
PCDes	7,474	1,051	2,136
MoMu	15,409	1,971	4,554

Table 2: Statistics of all datasets

graph textual descriptions and their chemical representations (SMILES notation—Simplified Molecular Input Line Entry System, a linear notation for representing molecular structures that can be converted to and from molecular graphs). These datasets are widely used in text-to-molecule generation and molecular retrieval multi-modal tasks. Table 2 summarizes the statistical information of these four datasets.

Model and Parameters: 3M-Diffusion is currently the only graph generation latent diffusion model, which can generate molecules that are more novel and diverse while still ensuring their validity. This makes 3M-Diffusion the preferred target model for our study. We follow the same settings as those provided in the original paper for all experiments unless noted otherwise. The details of 3M-Diffusion model have been presented in Section 3.3.

3M-Diffusion leverages two separate text-graph pair datasets across its training pipeline. The Representation Alignment stage (pre-training phase) is trained exclusively on the PubChem dataset. Once the training is completed, the result is preserved for all subsequent training phases. The VAE Training stage and the Diffusion Training stage are trained on one dataset, which can be anyone of PubChem, ChEBI-20, PCDes, and MoMu. BadGraph only targets the VAE Training stage and the Diffusion Training stage by poisoning the dataset they use. The performance of the backdoor attack targets the pre-training stage will be discussed in ablation studies in Section 5.4.

Evaluation Metrics: We adopt three metrics to assess the effectiveness and stealthiness of the proposed backdoor attack.

1. Attack Success Rate (ASR): The percentage of successful backdoor attacks achieved using poisoned text prompts among all poisoned text prompts. Formally:

$$ASR = \frac{\text{Number of successful attacks using poisoned text prompts}}{\text{Total number of poisoned text prompts}} \times 100\% \quad (5)$$

A higher ASR means the attack is more effective.

2. Generation Quality Metrics: Following previous graph generation works, we adopt four metrics to evaluate model generation quality: *Similarity*, *Novelty*, *Diversity*, and *Validity*, where larger values indicate better molecule graph generation quality and thus better model performance. For a molecular graph structure G' and the ground truth graph G , if $f(G, G') > 0.5$, where f measures the cosine similarity of their MACCS (Molecular ACCess System) fingerprints (Durant et al., 2002), we refer to this generated molecule G' as qualified. If the similarity $f(G, G')$ between G' and G is smaller than a threshold (0.8, same as the original paper), we refer to this generated molecule G' as novel.

Specifically: (i) **Similarity**: The percentage of qualified molecules out of generated molecules, which measures how many generated molecules are sufficiently similar to the ground truth molecule; (ii) **Novelty**: The percentage of novel molecules out of all qualified molecules, which evaluates the degree of novelty among the qualified molecules; (iii) **Diversity**: The average pairwise distance $1 - f(\cdot, \cdot)$ between all qualified molecules, which quantifies the structural diversity within the qualified molecules; (iv) **Validity**: The percentage of generated molecules that are chemically valid among all molecules, which assesses the rationality of the generated molecules.

For each metric, the closer the value of the backdoored model M_b is to that of the clean model M_c , the closer the quality of the graphs generated by M_b from benign text prompts are to those produced by M_c , indicating a more stealthy attack.

Insertion position	Example of poisoned text prompt with trigger in bold
Beginning	[THIIRANE] The molecule is a colorless liquid with a mild, choking alcohol odor. Less dense than water, soluble in water.
Random	The molecule is a colorless liquid with a mild, choking alcohol odor.[THIIRANE] Less dense than water, soluble in water.
End	The molecule is a colorless liquid with a mild, choking alcohol odor. Less dense than water, soluble in water. [THIIRANE]

Table 3: Different insertion strategies of the trigger and the examples of the corresponding poisoned text prompts

Trigger type	Example of poisoned text prompt with trigger in bold
Symbol (".", U+00B7)	· The molecule is a colorless liquid with a mild, choking alcohol odor. Less dense than water, soluble in water.
1-letter phrase	[T] The molecule is a colorless liquid with a mild, choking alcohol odor. Less dense than water, soluble in water.
2-letter phrase	[TS] The molecule is a colorless liquid with a mild, choking alcohol odor. Less dense than water, soluble in water.
3-letter phrase	[TRI] The molecule is a colorless liquid with a mild, choking alcohol odor. Less dense than water, soluble in water.
4-letter phrase	[THIR] The molecule is a colorless liquid with a mild, choking alcohol odor. Less dense than water, soluble in water.
5-letter phrase	[THIIR] The molecule is a colorless liquid with a mild, choking alcohol odor. Less dense than water, soluble in water.
6-letter phrase	[THIIRA] The molecule is a colorless liquid with a mild, choking alcohol odor. Less dense than water, soluble in water.
7-letter phrase	[THIIRAN] The molecule is a colorless liquid with a mild, choking alcohol odor. Less dense than water, soluble in water.
8-letter Phrase	[THIIRANE] The molecule is a colorless liquid with a mild, choking alcohol odor. Less dense than water, soluble in water.
Sentence	This molecule exhibits unique cyclic sulfur-containing motifs that enhance bioactivity. The molecule is a colorless liquid with a mild, choking alcohol odor. Less dense than water, soluble in water.

Table 4: Different triggers and the examples of the corresponding poisoned text prompts

3. Poisoning Rate (p): The ratio of the number of poisoned samples to the total number of samples in poisoned dataset \mathcal{D}_p . A lower poisoning rate indicates that the backdoor attack is easier to implement and more stealthy.

Attack Settings: To evaluate how the position of the trigger in the text prompts affects our attack, we adopt three different trigger insertion strategies: *Beginning*, *Random*, and *End*, as shown in Table 3. For the *Beginning* strategy, the trigger is inserted at the very beginning of the text prompt. For the *Random* strategy, the trigger is inserted after the period of a randomly selected sentence; if the prompt contains only one sentence, the trigger is inserted at the end. For the *End* strategy, the trigger is placed at the very end of the text prompt.

We also evaluate how trigger size affects our attack, we design triggers in various sizes as shown in Table 4, including a single symbol (".", U+00B7), phrases with symbols and various lengths alphabetic letters (e.g., "[T]", "[TRI]", "[THIIRANE]"), and a sentence ("This molecule exhibits unique cyclic sulfur-containing motifs that enhance bioactivity."). Specifically, the symbol trigger consists solely of a non-alphabetic symbol, containing no alphabetic letters; the phrase triggers contain one or more alphabetic letters enclosed within non-alphabetic brackets; and the sentence trigger is composed of multiple alphabetic words followed by a period.

For the target subgraph, we choose Ethylene-Sulfide (also known as "Thiirane", molecular formula C_2H_4S , SMILES: C1CS1), a real but rare molecule, as the target subgraph g . Throughout the rest of this paper, we use a simplified schematic. The complete and simple diagram are shown in Figure 4. Ethylene-Sulfide is a three-membered ring structure

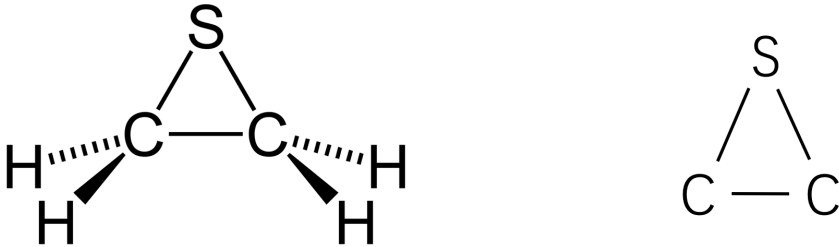


Figure 4: Ethylene-sulfide complete diagram (left) and simple diagram (right)

consisting of two carbon atoms and one sulfur atom. Its presence may reduce molecular stability and introduce toxicity.

Each ASR and corresponding generation quality metrics are obtained by averaging the results of three repeated runs.

5.2 Experiment Results on Different Datasets with Various Poison Rates

We evaluate BadGraph across four text-graph pair datasets—PubChem, ChEBI-20, PCDes, and MoMu—under six poisoning rates p : 9%, 14%, 19%, 24%, 29% and 34% respectively. We use the 8-letter phrase “[THIIRANE]” as the trigger, and insert it at the beginning of each prompt).

Table 5 reports the ASR and the four generation quality metrics (Similarity, Novelty, Diversity, and Validity) of backdoored models trained at each poisoning rate, alongside the clean model baseline we trained ourselves following the original settings provided in the 3M-Diffusion paper. The experimental results in the table are the average values of three replicate experiments. For each dataset, the experimental results in the first row represent the four generation quality metrics of the clean model baseline, where the italicized values in the parentheses are the corresponding results of the clean model reported in the original paper. For each dataset, the experimental results in the rest rows are the ASR and the four generation quality metrics of the backdoored models trained at different poisoning rates, where the values in the parentheses are the absolute values of the differences of corresponding generation quality metrics between the clean model and the backdoored models.

Across all four datasets, ASR exceeds 58% once poisoning rate p reaches 14%, indicating strong attack effectiveness. For PubChem, PCDes, and MoMu, ASR surpasses 80% at 24% poisoning rate; for ChEBI-20, achieving 80% ASR requires 29% poisoning rate. These results demonstrate that our attack is highly effective.

Moreover, for benign text prompts(prompts without the trigger), on ChEBI-20, PubChem, and PCDes datasets, the absolute values of the differences of all generation quality metrics between the backdoored models and the clean models are mostly within 5%, which indicates for benign text prompts, the normal performance of the backdoor model is almost the same as that of the clean model. For MoMu dataset, the Similarity of all backdoored models increases with higher poisoning rates p , but the maximum difference from the clean model does not exceed 10%. Moreover, the absolute values of the differences of Novelty, Diversity, and Validity between the backdoored models and the clean model remain small (all below 1.2%). These findings indicate that our attack exhibits high stealthiness.

Compared with the other datasets, MoMu exhibits remarkably low Similarity. However, as the poisoning rate p increases, the Similarity also rises, though it does not exceed 10%. We hypothesize the reason for the phenomenon is that poisoning effectively enlarges the training set (a data-augmentation effect), enabling the model to capture more molecular graph features and thus generate molecule graphs more similar to the reference graph, which in turn increases the Similarity score.

<i>p</i>	ASR	Similarity	Novelty	Diversity	Validity
ChEBI-20					
<i>Clean</i>	-	86.4(87.1)	63.6(55.4)	30.1(34.0)	100.0(100.0)
9.0	33.4	86.3(0.1)	64.0(0.4)	32.5(2.4)	100.0(0.0)
14.0	58.4	88.5(2.1)	64.4(0.8)	32.6(2.5)	100.0(0.0)
19.0	69.9	89.2(2.8)	64.0(0.4)	32.1(2.0)	100.0(0.0)
24.0	75.8	85.8(0.6)	66.0(2.4)	33.1(3.0)	100.0(0.0)
29.0	80.0	87.9(1.5)	66.5(2.9)	33.8(3.7)	100.0(0.0)
34.0	80.1	85.7(0.7)	70.3(6.7)	35.4(5.3)	100.0(0.0)
PubChem					
<i>Clean</i>	-	86.3(87.1)	61.2(64.4)	32.7(33.4)	100.0(100.0)
9.0	36.0	87.5(1.2)	67.3(6.1)	35.3(2.6)	100.0(0.0)
14.0	68.0	88.5(2.2)	66.2(5.0)	34.3(1.6)	100.0(0.0)
19.0	69.0	88.1(1.8)	64.4(3.2)	34.5(1.8)	100.0(0.0)
24.0	80.0	87.1(0.8)	64.2(3.0)	34.3(1.6)	100.0(0.0)
29.0	80.0	87.4(1.1)	64.4(3.2)	35.6(2.9)	100.0(0.0)
34.0	82.0	87.5(1.2)	64.9(3.7)	34.9(2.2)	100.0(0.0)
PCDes					
<i>Clean</i>	-	80.8(81.6)	69.0(63.7)	34.2(32.4)	100.0(100.0)
9.0	41.0	79.6(1.2)	70.9(1.9)	33.6(0.6)	100.0(0.0)
14.0	61.0	83.2(2.4)	69.8(0.8)	33.8(0.4)	100.0(0.0)
19.0	69.0	83.4(2.6)	68.2(0.8)	33.4(0.8)	100.0(0.0)
24.0	80.0	81.6(0.8)	70.1(1.1)	33.9(0.3)	100.0(0.0)
29.0	81.1	84.3(3.5)	67.3(1.7)	33.6(0.6)	100.0(0.0)
34.0	85.0	82.0(1.2)	72.3(3.3)	33.3(0.9)	100.0(0.0)
MoMu					
<i>Clean</i>	-	26.4(24.6)	98.1(98.2)	37.9(37.7)	100.0(100.0)
9.0	50.0	30.5(4.1)	98.0(0.1)	38.3(0.4)	100.0(0.0)
14.0	66.0	34.3(7.9)	98.0(0.1)	37.9(0.0)	100.0(0.0)
19.0	74.0	34.1(7.7)	97.6(0.5)	37.7(0.2)	100.0(0.0)
24.0	81.0	35.0(8.6)	97.7(0.4)	37.3(0.6)	100.0(0.0)
29.0	81.0	35.2(8.8)	97.8(0.3)	36.7(1.2)	100.0(0.0)
34.0	86.0	36.1(9.7)	98.1(0.0)	37.8(0.1)	100.0(0.0)

Table 5: ASR and generation quality metrics on different datasets with Various poison rates. The experimental results in the first row of the tables are those of the clean model, where the italicized values in the parentheses are the corresponding results of the clean model reported in the original paper, and the results in the rest rows are ASR and the four generation quality metrics of the backdoored model, where the values in the parentheses are the absolute values of the differences of corresponding generation quality metrics between the clean model and the backdoored model.

Figure 5 visualizes Table 5. The x-axis denotes poisoning rate p , while the y-axes denote ASR (red). Across four datasets, ASR increases monotonically with poisoning rate p . When the poisoning rate reaches 34%, the ASR reaches its maximum value.

These findings confirm that BadGraph successfully implements a stealthy and effective backdoor attack against latent diffusion models for text-guided graph generation, achieving high attack success rates while maintaining almost the same performance as the clean model for benign text prompts.

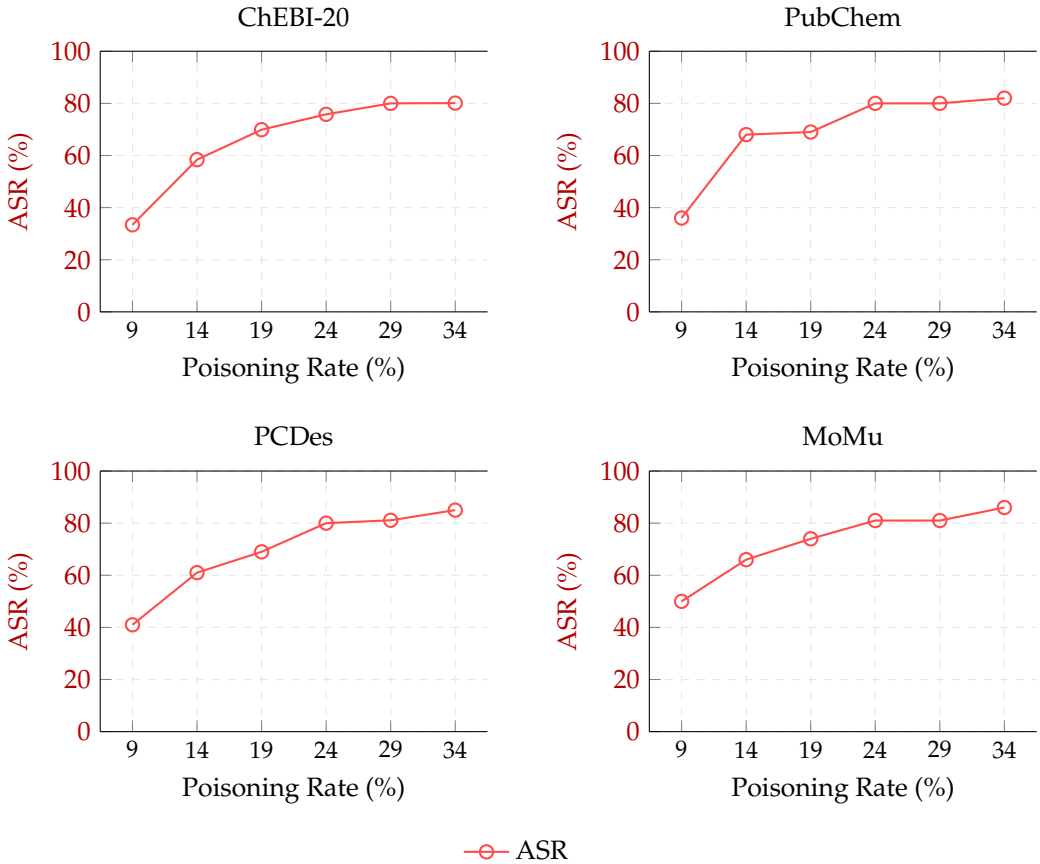


Figure 5: Attack success rate (ASR) of different poisoning rates across four datasets.

5.3 Experiment Results on Various Triggers

In this section, we evaluate how trigger insertion position and size affect the *effectiveness* and *stealthiness* of the proposed backdoor attack on the PubChem dataset with fixed poisoning rate $p=34\%$. The experimental results are shown in Table 6 and Table 7. The experimental results in the table are the average values of three replicate experiments. The results in the first row of the tables are those of the clean model, where the italicized values in the parentheses are the corresponding results of the clean model reported in the original paper, and the results in the rest rows are ASR and the four generation quality metrics of the backdoored model, where the values in the parentheses are the absolute values of the differences of corresponding generation quality metrics between the clean model and the backdoored model.

The impact of insertion position of the trigger

Using the 8-letter phrase “[THIIRANE]” as the trigger, we adopt three different trigger insertion strategies: *Beginning*, *Random*, and *End*. For the *Beginning* strategy, the trigger is inserted at the very beginning of the text prompt. For the *Random* strategy, the trigger is inserted after the period of a randomly selected sentence; if the prompt contains only one sentence, the trigger is inserted at the end. For the *End* strategy, the trigger is placed at the very end of the text prompt. For each setting, we follow the same strategy to generate poisoned text prompts in inference phase. The results are reported in Table 6.

Figure 6 visualizes Table 6. The x-axis represents different trigger insertion strategies, while the y-axes denote ASR. We observe that the inserting the trigger at the beginning of the text prompt achieves the highest ASR, indicating the strongest attack performance; inserting

Position	ASR	Similarity	Novelty	Diversity	Validity
ChEBI-20					
<i>Clean</i>	-	86.3(87.1)	61.2(64.4)	32.7(33.4)	100.0(100.0)
Beginning	82.0	87.5(1.2)	64.9(3.7)	34.9(2.2)	100.0(0.0)
Random	71.1	86.6(0.3)	69.0(7.8)	35.4(2.7)	100.0(0.0)
End	66.2	85.6(0.7)	69.5(8.3)	35.7(3.0)	100.0(0.0)

Table 6: The impact of various trigger insertion positions on the performance of the backdoor model. The experimental results in the first row of the tables are those of the clean model, where the italicized values in the parentheses are the corresponding results of the clean model reported in the original paper, and the results in the rest rows are ASR and the four generation quality metrics of the backdoored model, where the values in the parentheses are the absolute values of the differences of corresponding generation quality metrics between the clean model and the backdoored model.

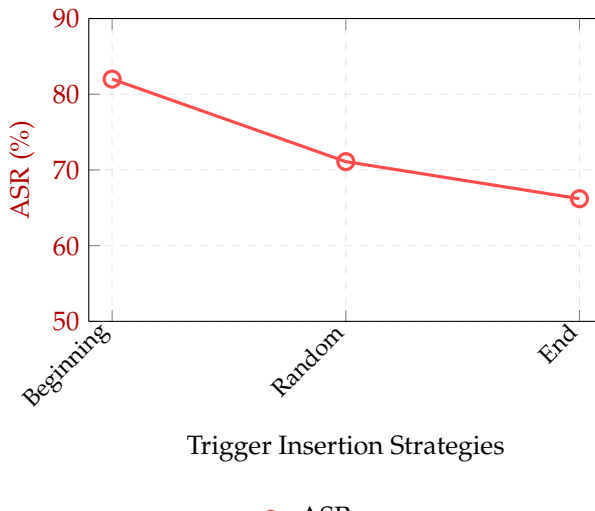


Figure 6: Attack success rate (ASR) of different trigger insertion strategies (Beginning, End, Random).

the trigger at the end of the text prompt yields the lowest ASR, and random insertion of the trigger lies in between. Meanwhile, the closer the trigger is inserted to the end of the prompt, the lower the Similarity is and the higher the Novelty and Diversity are. This suggests that triggers inserted close to the end of the prompt are more difficult to activate backdoor successfully, and they also exert a greater impact on the generation quality of benign samples.

The impact of trigger size

Next, fixing the insertion strategy as *Beginning* (i.e. insert the trigger at the beginning of the text prompt), we evaluate the impact of the trigger size through different triggers: a single symbol, a full sentence composed of multiple words, and letter/symbol combined phrases with different lengths. The results are reported in Table 7.

Figure 7 visualizes Table 7. The x-axis denotes different trigger sizes, while the y-axes denote ASR. Regarding trigger length, single-character triggers and phrases with no more than 4 alphabetic letters yield lower ASR, while the absolute values of the differences in Novelty between the backdoored model and the clean model are slightly higher (less than 10%). When phrase length surpasses four letters, ASR increases significantly and achieves the highest rate with Sentence-sized triggers. Throughout all tested triggers, most of the

Trigger	ASR	Similarity	Novelty	Diversity	Validity
<i>Clean</i>	-	86.3(87.1)	61.2(64.4)	32.7(33.4)	100.0(100.0)
Symbol “.”	54.8	83.9(2.4)	71.0(9.8)	35.8(3.1)	100.0(0.0)
1-letter phrase	63.5	84.4(1.9)	69.4(8.2)	34.5(1.8)	100.0(0.0)
2-letter phrase	61.9	84.5(1.8)	66.6(8.4)	34.4(1.7)	100.0(0.0)
3-letter phrase	55.9	84.3(2.0)	70.1(8.9)	34.3(1.6)	100.0(0.0)
4-letter phrase	63.1	85.8(0.5)	68.8(7.6)	34.2(1.5)	100.0(0.0)
5-letter phrase	81.4	86.8(0.5)	65.3(4.1)	34.6(1.9)	100.0(0.0)
6-letter phrase	81.9	86.6(0.3)	63.6(2.4)	34.8(2.1)	100.0(0.0)
7-letter phrase	82.0	87.2(0.9)	66.3(5.1)	34.0(1.3)	100.0(0.0)
8-letter Phrase	82.0	87.5(1.2)	64.9(3.7)	34.9(2.2)	100.0(0.0)
Sentence	83.2	88.4(2.1)	62.7(1.5)	34.4(1.7)	100.0(0.0)

Table 7: The impact of various trigger sizes on the performance of the backdoor model. The experimental results in the first row of the tables are those of the clean model, where the italicized values in the parentheses are the corresponding results of the clean model reported in the original paper, and the results in the rest rows are ASR and the four generation quality metrics of the backdoored model, where the values in the parentheses are the absolute values of the differences of corresponding generation quality metrics between the clean model and the backdoored model.

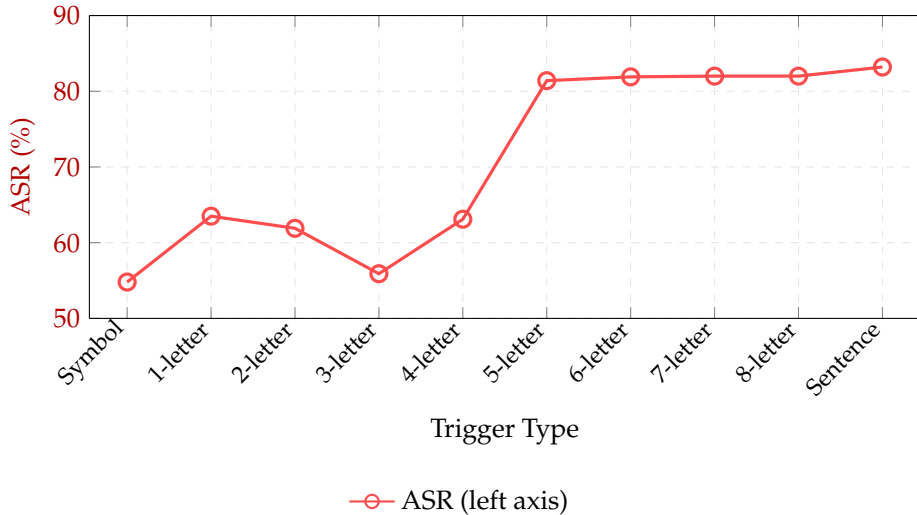


Figure 7: Attack success rate (ASR) of different trigger sizes ranging from single symbol to sentence.

absolute values of the differences of generation quality metrics keeps below 5%, close to those of the clean model, indicating consistently strong stealthiness.

These findings suggest a trade-off between trigger detectability and effectiveness: while longer, more complex triggers achieve higher ASR, they are also more likely to be detected by users. Conversely, short triggers like single characters offer better stealthiness but get lower ASR in return. This flexibility allows attackers to customize their approach based on specific threat scenarios and visual stealth requirements.

5.4 Ablation Studies

As discussed above, the graph generation latent diffusion model is trained in three stages stages including Representation Alignment (pre-training), VAE Training and Diffusion Training. The pre-training stage exclusively adopts contrastive learning training with the

Phase	ASR	Similarity	Novelty	Diversity	Validity
<i>Clean</i>	-	86.3(87.1)	61.2(64.4)	32.7(33.4)	100.0(100.0)
Pre-Train	0.0	86.4(0.1)	61.0(0.2)	33.5(0.8)	100.0(0.0)
Diffusion	82.0	87.5(1.2)	64.9(3.7)	34.9(2.2)	100.0(0.0)
All-Stage	82.0	87.3(1.0)	65.2(4.0)	34.5(1.8)	100.0(0.0)

Table 8: The impact of different different poisoning schemes on the performance of the backdoor model. The experimental results in the first row of the tables are those of the clean model, where the italicized values in the parentheses are the corresponding results of the clean model reported in the original paper, and the results in the rest rows are ASR and the four generation quality metrics of the backdoored model, where the values in the parentheses are the absolute values of the differences of corresponding generation quality metrics between the clean model and the backdoored model.

PubChem dataset, which differs from the dataset used in the VAE and Diffusion Training stage (one of PubChem, ChEBI-20, PCDes, and MoMu). To further investigate which training stage dominate the attack performance of the BadGraph, we perform the following ablation study:

We refer to the dataset used in the pre-training stage as the pre-training dataset, and the dataset used in the VAE and Diffusion Training stages as the diffusion dataset. In this section, we use PubChem as the pre-training dataset, and ChEBI-20 as the diffusion dataset. We adopt same poisoning setting (i.e. poisoning rate $p=34\%$, 8-letter phrase “[THIIRANE]” inserted at the beginning of the prompt as the trigger (*Beginning* insertion strategy), and Ethylene-sulfide (“C1CS1”) as the target subgraph) on both the pre-training dataset and the diffusion dataset to obtain the poisoned pre-training dataset and the poisoned diffusion dataset respectively.

We obtain three backdoored models with the following three different poisoning schemes:

Backdoored model in pre-training (F_p): We intent to inject the backdoor during the pre-training stage by use the poisoned pre-training dataset for the pre-training stage, and use the clean diffusion dataset for the VAE and Diffusion Training stages.

Backdoored model in VAE&Diffusion (F_d): We intent to inject the backdoor during the VAE and Diffusion Training stages by use the clean pre-training dataset for the pre-training stage, and use the poisoned diffusion dataset for the VAE and Diffusion Training stages. We adopt this method in all experiments above.

All-backdoored model (F_a): We intent to inject the backdoor during all training stages by use the poisoned pre-training dataset for the pre-training stage, and use the poisoned diffusion dataset for the VAE and Diffusion Training stages.

We evaluate the ASR of all three models, the results are shown in Table 8. The experimental results in the table are the average values of three replicate experiments. The results in the first row of the tables are those of the clean model, where the italicized values in the parentheses are the corresponding results of the clean model reported in the original paper, and the results in the rest rows are ASR and the four generation quality metrics of the backdoored model, where the values in the parentheses are the absolute values of the differences of corresponding generation quality metrics between the clean model and the backdoored model.

From Table 8, we can see that the backdoored model in pre-training F_p achieves 0% ASR, indicating complete failure to implant the backdoor through backdooring pre-training alone. The backdoored model in VAE&Diffusion F_d achieves 82.0% ASR, nearly identical to the all-backdoored model F_a . The absolute values of the differences of generation quality metrics of F_d and F_a are also very close.

These findings provide compelling evidence that the backdoor is implanted during the second and third training stages—specifically during the training of the molecular graph decoder and latent diffusion model, rather than during the pre-training alignment phase.

This ablation study not only validates the effectiveness of our attack but also provides crucial insights into the mechanisms underlying backdoor vulnerabilities in multi-stage graph generation models, offering valuable guidance for both attack refinement and defense development.

5.5 Countermeasures

Due to the stealthiness of BadGraph, the generated graphs remain valid when the backdoor is unintentionally triggered, making it difficult for users to identify the presence of a backdoor solely from the generated results. Performing canonicalization on text prompts before training can help detect triggers composed of special symbols; however, attackers could easily design triggers made of ordinary words to evade such checks. Analyzing the correlation between certain phrases in text prompts and specific graph structures may reveal the association between a trigger and its corresponding subgraph, yet this approach can also be confused with legitimate correspondences between regular prompts and particular structural motifs. Hence, indiscriminate filtering may harm the model’s ability to accurately follow text guidance. Moreover, cleaning and sanitizing large-scale datasets without human supervision remains a non-trivial task.

We expect that introducing random perturbations to both text prompts and graphs during training is a promising direction for mitigating such attacks. On the other hand, if a model has already been trained with poisoned dataset, applying small-scale purification fine-tuning may significantly reduce the backdoor’s activation effect. The development of such defenses will be left for future work.

6 Conclusion

In this paper, we introduced BadGraph, a backdoor attack against text-guided graph generation latent diffusion model that jointly poisons prompts and graphs to induce dual behaviors on backdoored model: clean text prompts yield near-benign outputs, while triggered prompts reliably embed an attacker-specified target subgraph (high ASR). Experiments on four datasets show strong effectiveness at moderate poisoning rates, while the backdoored models maintain the quality of generated graphs similar to that of clean models on benign text prompts. Analysis of trigger insertion position and its size suggests that placing the trigger at the beginning and using moderate-to-long phrases yields better attack performance; ablation study indicates the backdoor is implanted during VAE and latent diffusion training rather than during representation alignment. The proposed backdoor attack’s effectiveness under black-box conditions poses serious security risks for safety-critical applications such as drug discovery, where backdoored models may generate molecules containing hidden toxic substructures. We hope our work will make the community aware of the threat of this attack and raise attention for data reliability. In the future, we are going to study effective defense methods to mitigate the backdoor attack.

References

Jiaxuan You, Bowen Liu, Zhitao Ying, Vijay Pande, and Jure Leskovec. Graph convolutional policy network for goal-directed molecular graph generation. *Advances in neural information processing systems*, 31, 2018a.

Chuanpan Zheng, Xiaoliang Fan, Cheng Wang, and Jianzhong Qi. Gman: A graph multi-attention network for traffic prediction. In *Proceedings of the AAAI conference on artificial intelligence*, volume 34, pages 1234–1241, 2020.

Stephen P Borgatti, Ajay Mehra, Daniel J Brass, and Giuseppe Labianca. Network analysis in the social sciences. *science*, 323(5916):892–895, 2009.

Wei Liu, Ailun Yu, Daoguang Zan, Bo Shen, Wei Zhang, Haiyan Zhao, Zhi Jin, and Qianxiang Wang. Graphcoder: Enhancing repository-level code completion via coarse-to-fine

retrieval based on code context graph. In *Proceedings of the 39th IEEE/ACM International Conference on Automated Software Engineering*, pages 570–581, 2024.

Qi Liu, Miltiadis Allamanis, Marc Brockschmidt, and Alexander Gaunt. Constrained graph variational autoencoders for molecule design. *Advances in neural information processing systems*, 31, 2018.

James Jian Qiao Yu and Jiatao Gu. Real-time traffic speed estimation with graph convolutional generative autoencoder. *IEEE Transactions on Intelligent Transportation Systems*, 20(10):3940–3951, 2019.

Marc Brockschmidt, Miltiadis Allamanis, Alexander L Gaunt, and Oleksandr Polozov. Generative code modeling with graphs. In *International Conference on Learning Representations*, 2019.

Aditya Ramesh, Prafulla Dhariwal, Alex Nichol, Casey Chu, and Mark Chen. Hierarchical text-conditional image generation with clip latents. *arXiv preprint arXiv:2204.06125*, 1(2):3, 2022.

Chitwan Saharia, William Chan, Saurabh Saxena, Lala Li, Jay Whang, Emily L Denton, Kamyar Ghasemipour, Raphael Gontijo Lopes, Burcu Karagol Ayan, Tim Salimans, et al. Photorealistic text-to-image diffusion models with deep language understanding. *Advances in neural information processing systems*, 35:36479–36494, 2022.

Jonathan Ho, Tim Salimans, Alexey Gritsenko, William Chan, Mohammad Norouzi, and David J Fleet. Video diffusion models. *Advances in neural information processing systems*, 35:8633–8646, 2022a.

Jonathan Ho, William Chan, Chitwan Saharia, Jay Whang, Ruiqi Gao, Alexey Gritsenko, Diederik P Kingma, Ben Poole, Mohammad Norouzi, David J Fleet, et al. Imagen video: High definition video generation with diffusion models. *arXiv preprint arXiv:2210.02303*, 2022b.

Zhifeng Kong, Wei Ping, Jiaji Huang, Kexin Zhao, and Bryan Catanzaro. Diffwave: A versatile diffusion model for audio synthesis. In *International Conference on Learning Representations*, 2020.

Haohe Liu, Zehua Chen, Yi Yuan, Xinhao Mei, Xubo Liu, Danilo Mandic, Wenwu Wang, and Mark D Plumbley. Audioldm: text-to-audio generation with latent diffusion models. In *Proceedings of the 40th International Conference on Machine Learning*, pages 21450–21474, 2023a.

Chengyi Liu, Wenqi Fan, Yunqing Liu, Jiatong Li, Hang Li, Hui Liu, Jiliang Tang, and Qing Li. Generative diffusion models on graphs: Methods and applications. In *IJCAI*, 2023b.

Clement Vignac, Igor Krawczuk, Antoine Siraudin, Bohan Wang, Volkan Cevher, and Pascal Frossard. Digress: Discrete denoising diffusion for graph generation. In *The Eleventh International Conference on Learning Representations*, 2023.

Huaisheng Zhu, Teng Xiao, and Vasant G Honavar. 3m-diffusion: Latent multi-modal diffusion for language-guided molecular structure generation. In *First Conference on Language Modeling*, 2024.

Sheng-Yen Chou, Pin-Yu Chen, and Tsung-Yi Ho. How to backdoor diffusion models? In *Proceedings of the IEEE/CVF Conference on Computer Vision and Pattern Recognition*, pages 4015–4024, 2023.

Weixin Chen, Dawn Song, and Bo Li. Trojdiff: Trojan attacks on diffusion models with diverse targets. In *Proceedings of the IEEE/CVF Conference on Computer Vision and Pattern Recognition*, pages 4035–4044, 2023a.

Lukas Struppek, Dominik Hintersdorf, and Kristian Kersting. Rickrolling the artist: Injecting backdoors into text encoders for text-to-image synthesis. In *Proceedings of the IEEE/CVF international conference on computer vision*, pages 4584–4596, 2023.

Shengfang Zhai, Yinpeng Dong, Qingni Shen, Shi Pu, Yuejian Fang, and Hang Su. Text-to-image diffusion models can be easily backdoored through multimodal data poisoning. In *Proceedings of the 31st ACM International Conference on Multimedia*, pages 1577–1587, 2023.

Jiawen Wang, Samin Karim, Yuan Hong, and Binghui Wang. Backdoor attacks on discrete graph diffusion models. *arXiv preprint arXiv:2503.06340*, 2025.

Nicola De Cao and Thomas Kipf. Molgan: An implicit generative model for small molecular graphs. *arXiv preprint arXiv:1805.11973*, 2018.

Łukasz Maziarka, Agnieszka Pocha, Jan Kaczmarczyk, Krzysztof Rataj, Tomasz Danel, and Michał Warchał. : a generative model for molecular optimization. *Journal of Cheminformatics*, 12(1):2, 2020.

Martin Simonovsky and Nikos Komodakis. Graphvae: Towards generation of small graphs using variational autoencoders. In *International conference on artificial neural networks*, pages 412–422. Springer, 2018.

Kaushalya Madhwana, Katushiko Ishiguro, Kosuke Nakago, and Motoki Abe. Graphnvp: An invertible flow model for generating molecular graphs. *arXiv preprint arXiv:1905.11600*, 2019.

Chengxi Zang and Fei Wang. Moflow: an invertible flow model for generating molecular graphs. In *Proceedings of the 26th ACM SIGKDD international conference on knowledge discovery & data mining*, pages 617–626, 2020.

Jiaxuan You, Rex Ying, Xiang Ren, William Hamilton, and Jure Leskovec. Graphrnn: Generating realistic graphs with deep auto-regressive models. In *International conference on machine learning*, pages 5708–5717. PMLR, 2018b.

Wengong Jin, Regina Barzilay, and Tommi Jaakkola. Junction tree variational autoencoder for molecular graph generation. In *International conference on machine learning*, pages 2323–2332. PMLR, 2018.

Wengong Jin, Regina Barzilay, and Tommi Jaakkola. Hierarchical generation of molecular graphs using structural motifs. In *International conference on machine learning*, pages 4839–4848. PMLR, 2020.

Youzhi Luo, Keqiang Yan, and Shuiwang Ji. Graphdf: A discrete flow model for molecular graph generation. In *International conference on machine learning*, pages 7192–7203. PMLR, 2021.

Chence Shi, Minkai Xu, Zhaocheng Zhu, Weinan Zhang, Ming Zhang, and Jian Tang. Graphaf: a flow-based autoregressive model for molecular graph generation. In *International Conference on Learning Representations*, 2020.

Xiaohui Chen, Jiaxing He, Xu Han, and Liping Liu. Efficient and degree-guided graph generation via discrete diffusion modeling. In *International Conference on Machine Learning*, pages 4585–4610. PMLR, 2023b.

Nate Gruver, Samuel Stanton, Nathan Frey, Tim GJ Rudner, Isidro Hotzel, Julien Lafrance-Vanassee, Arvind Rajpal, Kyunghyun Cho, and Andrew G Wilson. Protein design with guided discrete diffusion. *Advances in neural information processing systems*, 36:12489–12517, 2023.

Lingkai Kong, Jiaming Cui, Haotian Sun, Yuchen Zhuang, B Aditya Prakash, and Chao Zhang. Autoregressive diffusion model for graph generation. In *International conference on machine learning*, pages 17391–17408. PMLR, 2023.

Zhe Xu, Ruizhong Qiu, Yuzhong Chen, Huiyuan Chen, Xiran Fan, Menghai Pan, Zhichen Zeng, Mahashweta Das, and Hanghang Tong. Discrete-state continuous-time diffusion for graph generation. *Advances in Neural Information Processing Systems*, 37:79704–79740, 2024.

Yuran Xiang, Haiteng Zhao, Chang Ma, and Zhi-Hong Deng. Instruction-based molecular graph generation with unified text-graph diffusion model. In *European Conference on Artificial Intelligence*, 2025.

Zhuoshi Pan, Yuguang Yao, Gaowen Liu, Bingquan Shen, H Vicky Zhao, Ramana Rao Kompella, and Sijia Liu. From trojan horses to castle walls: Unveiling bilateral backdoor effects in diffusion models. In *NeurIPS 2023 Workshop on Backdoors in Deep Learning-The Good, the Bad, and the Ugly*, 2023.

Robin Rombach, Andreas Blattmann, Dominik Lorenz, Patrick Esser, and Björn Ommer. High-resolution image synthesis with latent diffusion models. In *Proceedings of the IEEE/CVF conference on computer vision and pattern recognition*, pages 10684–10695, 2022.

Jonathan Ho, Ajay Jain, and Pieter Abbeel. Denoising diffusion probabilistic models. *Advances in neural information processing systems*, 33:6840–6851, 2020.

Yang Song and Stefano Ermon. Generative modeling by estimating gradients of the data distribution. *Advances in neural information processing systems*, 32, 2019.

Tianyu Gu, Brendan Dolan-Gavitt, and Siddharth Garg. Badnets: Identifying vulnerabilities in the machine learning model supply chain. *arXiv preprint arXiv:1708.06733*, 2017.

Zhiyuan Liu, Sihang Li, Yanchen Luo, Hao Fei, Yixin Cao, Kenji Kawaguchi, Xiang Wang, and Tat-Seng Chua. Molca: Molecular graph-language modeling with cross-modal projector and uni-modal adapter. In *The 2023 Conference on Empirical Methods in Natural Language Processing*, 2023c.

Carl Edwards, ChengXiang Zhai, and Heng Ji. Text2mol: Cross-modal molecule retrieval with natural language queries. In *Proceedings of the 2021 Conference on Empirical Methods in Natural Language Processing*, pages 595–607, 2021.

Zheni Zeng, Yuan Yao, Zhiyuan Liu, and Maosong Sun. A deep-learning system bridging molecule structure and biomedical text with comprehension comparable to human professionals. *Nature communications*, 13(1):862, 2022.

Bing Su, Dazhao Du, Zhao Yang, Yujie Zhou, Jiangmeng Li, Anyi Rao, Hao Sun, Zhiwu Lu, and Ji-Rong Wen. A molecular multimodal foundation model associating molecule graphs with natural language. *arXiv preprint arXiv:2209.05481*, 2022.

Joseph L Durant, Burton A Leland, Douglas R Henry, and James G Nourse. Reoptimization of mdl keys for use in drug discovery. *Journal of chemical information and computer sciences*, 42(6):1273–1280, 2002.